A NEW BIS-TRÖGER'S BASE: SYNTHESIS, SPECTROSCOPY, CRYSTAL STRUCTURE AND ISOMERIZATION

Martin VALÍK[a1], Pavel MATĚJKA[a2], Eberhardt HERDTWECK[b], Vladimír KRÁL[a3] and Bohumil DOLENSKÝ[a4,*]

[a] *Department of Analytical Chemistry, Institute of Chemical Technology, Prague, Technická 5, 166 28 Prague 6, Czech Republic; e-mail:* [1] *valik@vscht.cz,* [2] *pavel.matejka@vscht.cz,* [3] *kralv@vscht.cz,* [4] *dolenskb@vscht.cz*

[b] *Department of Inorganic Chemistry, Technische Universität München, Lichtenbergstraße 4, D-85747 Garching, Germany; e-mail: eberhardt.herdtweck@ch.tum.de*

Received August 2, 2006
Accepted August 14, 2006

A new bis-Tröger's base was prepared from a tetraamine precursor as a mixture of two diastereoisomers. One of the isomers has a chair-like geometry, and the other possesses a boat-like geometry, embodying molecular tweezers. A one-pot preparation of bis-TB isomers and their interconversion under acid conditions was also studied. Structures of both isomers were confirmed by single-crystal X-ray diffraction. Extensive spectroscopic data, including ^{1}H and ^{13}C NMR, IR and Raman spectra of the isomers, are given.

Keywords: Molecular tweezers; Tröger's bases; Chiral receptors; Isomerization; IR/Raman spectroscopy; NMR spectroscopy; X-ray diffraction.

In 1887, Tröger described[1] the condensation of *p*-toluidine with formaldehyde to afford an unknown base. It was not until 1935 that Spielman solved[2] its structure. He found that the base is a unique compound, which possessed nitrogens which do not undergou umbrella inversion. The compound, today known as Tröger's base (TB), became simply known as an example of a "chiral nitrogen" compound, which is stable at room temperature for long periods. In the late 1990's supramolecular chemists started a renaissance of TB compounds. TB derivatives once being curiosities in organic chemistry textbooks become building blocks for molecular architects. The reasons for their rediscovery are the rigid V-shape (85–120°) and, of course, their inherent chirality. Thus, TB derivatives found use in supramolecular chemistry[3], with applications including the construction of receptors for achiral[4] and chiral[5] analytes, as well as for drug development[6].

A few years ago, TB derivatives of new dimensionality were discovered by the findings[7,8] that more than one TB system (1,5-diazabicyclo[3.3.1]-

doi:10.1135/cccc20061278

nonane) can be attached to a single central benzene ring. The preparation of bis-TB derivatives via procedures, in which each TB system is formed in a separate reaction, was described[7]. We have published an all-TB-at-once procedure, in which two or even three TB frameworks are formed in one step[8]. In addition, we have recently published a one-pot mixed condensation of a monoamine with a diamine, in which bis-TB derivatives (and higher-order linear oligo-TB derivatives) are formed without intermediate preparation[9].

The bis-TB derivatives exist as boat-like (*syn*-bis-TB) and chair-like (*anti*-bis-TB) diastereoisomers, which can be interconverted under acid conditions. The *syn*-bis-TB isomer mimics chiral molecular tweezers. Thus, it is an interesting subject for supramolecular chemistry. In this paper we described the preparation of new bis-TB derivatives in good yields. We also describe a first demonstration of their binding ability, stability in acid media, and spectral properties useful in distinguishing between the *syn* and *anti* isomers.

Preparation of Bis-TB

Acylation of 1,4-diaminobenzene with 4-methoxy-2-nitrobenzoyl chloride produced bisamide **1**. Reduction of the nitro groups followed by the amide reduction with $LiAlH_4$ afforded tetraamine **3**, the precursor for the concomitant formation of two TB frameworks[8]. The reaction of **3** with a source of formaldehyde in acid media can give two possible regioisomers, **4** and **5** (Scheme 1 and Chart 1). Nevertheless, we found that regioisomer **4** is formed exclusively as a mixture of two diastereoisomers (Fig. 1), the *anti* diastereoisomer **4a** (racemic mixture) and *syn* diastereoisomer **4b** (*meso*-form), in the 5:3 ratio. Each diastereoisomer was isolated and their structures were confirmed by single-crystal X-ray diffraction (Figs 2 and 3). Their regioselectivity is surprising; however, it is in full accordance with the current state-of-the-art in this field[7–10a]. The yield of bis-TB **4** was 40% (25% of **4a** and 15% of **4b**, overall yield 35%), which is dramatically better than we obtained[8] with aniline derivatives (ca. 5%). This is apparently due to the blocking of the positions *para* to the NH_2 groups with methoxy groups, which prevents oligomer-forming side reactions.

In addition, we tried to prepare bis-TB **4** by the mixed condensation of 4-methoxyaniline and 1,4-phenylenediamine with hexamethylentetramine (HMTA) in TFA, i.e. by the oligomerization reaction we recently published[9]. Under these conditions we isolated the expected isomers of bis-TB **4** in 7% yield (**4a**/**4b** 2:1). Dimethoxy-TB derivative **6** (19%) and its formylated derivative **7** (2%) were also isolated (Chart 1).

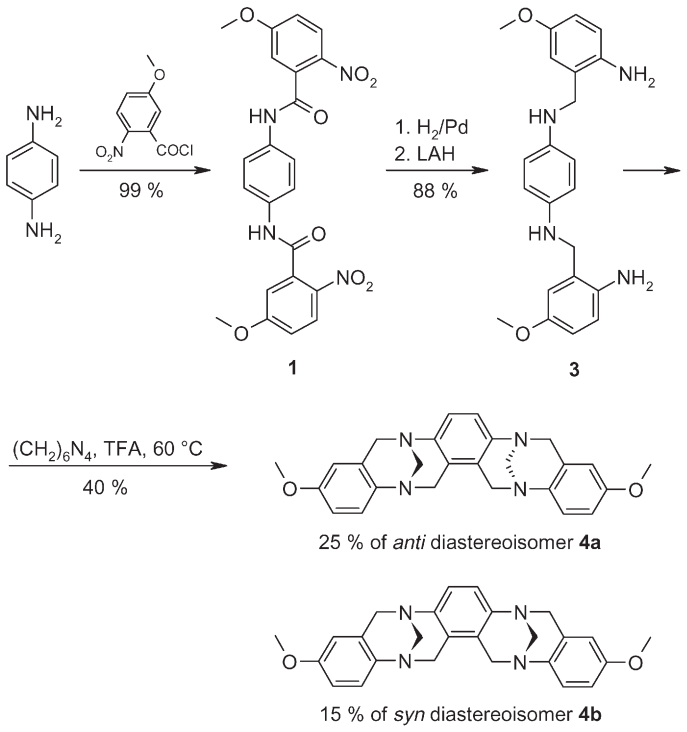

SCHEME 1
Synthesis of bis-Tröger's bases **4a** and **4b**

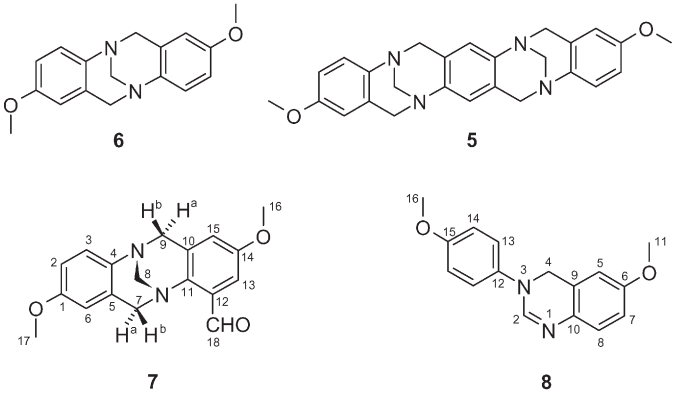

CHART 1

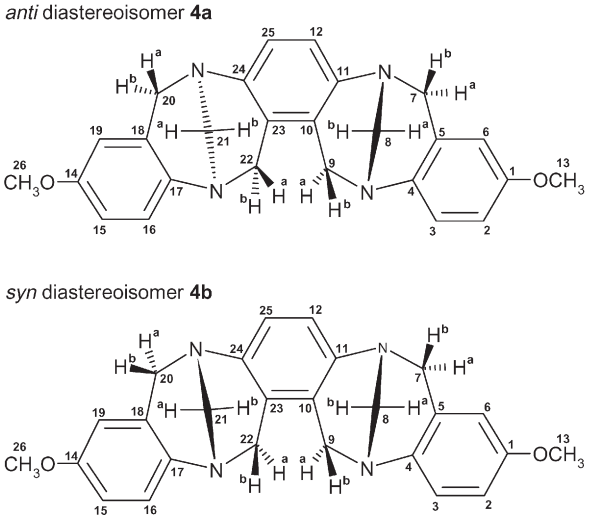

FIG. 1
Diastereoisomers **4a** and **4b**, numbering for NMR assignments

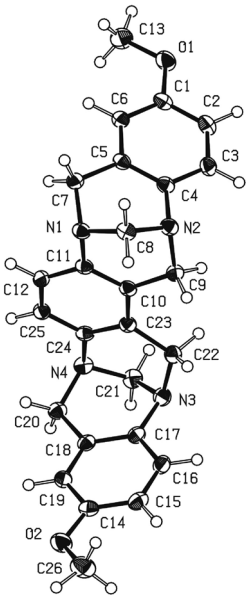

FIG. 2
ORTEP style plot of *anti* diastereoisomer **4a**. Thermal ellipsoids are drawn at the 50% probability level (crystal methanol is omitted)

Next, we tried the oligomerization of 4-methoxyaniline and 1,4-phenylenediamine with paraformaldehyde in the melt containing TsOH. We observed no formation of bis-TB **4**, and even no formation of TB **6**. The only isolated product was quinazoline **8** (20% yield). Quinazoline **8** is also formed in a similar yield (22%) when only 4-methoxyaniline and paraformaldehyde were melted with TsOH (i.e. without 1,4-phenylenediamine). Note that quinazoline **8** is described[11] as the product of reaction 4-methoxyaniline with formaldehyde in aqueous acids (yield 22%).

Nuclear Magnetic Resonance

For many studies it would be useful to have the unambiguous assignment of the chemical shifts of atoms of **4a** and **4b**, and also a universal and fast method to distinguish between *anti* diastereoisomer **4a** and *syn* diastereoisomer **4b** without X-ray analysis. The chemical shifts were assigned analysis of 1D and 2D NMR spectra. Structural parameters were also obtained from computer models of the isomers of **4**. The geometries were op-

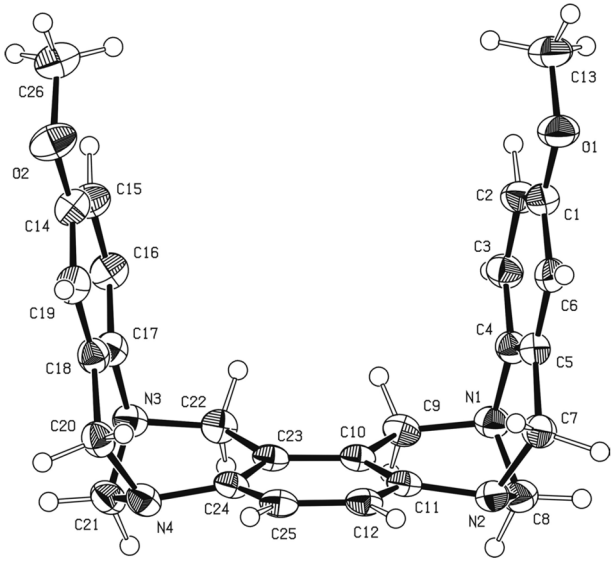

FIG. 3
ORTEP style plot of *syn* diastereoisomer **4b** in the solid state. Thermal ellipsoids are drawn at the 50% probability level. Selected contact distances: O1···O2 8.166(2) Å; Cg1···Cg2 7.038 Å. Cg defines the center of gravity of the periphery aromatic rings

timized by PM3 semiempirical method using HyperChem 6.03 software. Thus, the distances between hydrogen atoms from computer models and from the single-crystal X-ray structures aided to explain the observed NOEs (Table I). Similarly, the dihedral angles were used to calculate the coupling constants from the Karplus relationship $^3J_{CH} = 3.6 \cos 2\theta - \cos \theta + 4.3$ for a better understanding of HMBC spectra, where the intensity of the correlation peak is proportional to the value of interaction constant (Table II). The assignment of many of the signals in the ^{13}C and ^1H NMR spectra was relatively straightforward. However, the assignment of certain specific TB framework protons, namely H^{7a}, H^{7b}, H^{8a}, H^{8b}, H^{9a}, H^{9b} (Fig. 1), was challenging. The following findings hold for both isomers of **4** as well as for previously published TB derivatives[7–9,12].

Due to the shorter distance of H^{7a}–H^6 compared to H^{7b}–H^6, a significantly stronger NOE at H^{7a} compared to H^{7b} was observed when H^6 was irradiated in the NOESY experiment. Similarly, the NOE was observed only at H^{7a} when H^{12} was irradiated. In addition, the assignment was in accord with the expected value of $^3J_{CH}$ of C^8–H^{7a} and C^8–H^{7b}, wherein strong correlation of C^8 was observed with H^{7a} but no correlation with H^{7b} in the HMBC spec-

TABLE I
Selected atom distances (in Å) in **4a** and **4b**, and the intensity of observed NOE

Distance	*anti* Diastereoisomer **4a**			*syn* Diastereoisomer **4b**		
	model[a]	X-ray	NOE[b]	model[a]	X-ray	NOE[b]
H^6–H^{7a}	2.63	2.55(2)	m	2.61	2.53(3)	m
H^6–H^{7b}	2.81	2.83(2)	w	2.79	3.00(3)	w
H^{8a}–H^{7b}	2.61	2.39(2)	w	2.61	2.33(3)	w
H^{8b}–H^{7b}	3.75	3.48(2)	null	3.75	3.52(3)	null
H^{8b}–H^{9b}	2.61	2.39(2)	w	2.62	2.36(3)	w
H^{8a}–H^{9b}	3.75	3.48(2)	null	3.76	3.52(3)	null
H^3–H^{9a}	2.73	2.58(2)	m	2.73	2.50(3)	m
H^3–H^{9b}	3.71	3.65(2)	null	3.71	3.65(3)	null
H^{12}–H^{7a}	2.70	2.51(2)	m	2.71	2.51(3)	m
H^{12}–H^{7b}	3.68	3.60(2)	null	3.69	3.68(3)	null

[a] PM3 optimized structure (vide infra). [b] NOE intensity is given in the scale strong > medium > weak > null.

tra. Next, in the HMBC spectrum, C^{11} has a strong correlation only with H^{7b}. Note that a stronger correlation peak is observed between H^6 and H^{7b} than between H^6 and H^{7a} in the COSY spectrum. By analogy to protons H^7, irradiation of H^3 gives rise to a NOE only on H^{9a} and not on H^{9b}. A strong correlation was observed for C^8–H^{9a} and null correlation for C^8–H^{9b} in the HMBC spectrum. C^4 shows a strong correlation in the HMBC spectrum only with H^{9b}. Irradiating H^{8a} gives a NOE at H^{7b}, while irradiation of H^{8b} affords a NOE at H^{9b}. It is also very helpful that in the HMBC spectrum, both C^4 and C^7 have stronger correlations with H^{8b} than with H^{8a}, whereas both carbons C^{11} and C^9 show stronger correlations with H^{8a} than with H^{8b}, in

TABLE II
Selected dihedral angles (in °) and the intensity of observed HMBC cross-peaks

Angle	*anti* Diastereoisomer **4a**				*syn* Diastereoisomer **4b**			
	model[a]	X-ray	$^3J_{CH}$	HMBC[b]	model[a]	X-ray	$^3J_{CH}$	HMBC[b]
C^8–N–C^7–H^{7a}	163.8	169.8(9)	8.3	s	163.6	171.5(11)	8.3	s
C^8–N–C^7–H^{7b}	–80.9	–72.4(10)	0.7	null	–81.1	–70.8(11)	0.7	null
C^8–N–C^9–H^{9a}	163.5	170.1(10)	8.3	s	163.3	168.7(12)	8.3	s
C^8–N–C^9–H^{9b}	–81.5	–73.8(9)	0.7	null	–81.7	–73.6(12)	0.7	null
C^4–N–C^8–H^{8a}	–62.5	–66.8(10)	1.8	w	–62.5	–68.8(12)	1.8	w
C^4–N–C^8–H^{8b}	178.8	174.5(9)	8.9	s	178.8	169.3(11)	8.9	s
C^4–C^5–C^7–H^{7a}	129.4	–135.3(9)	4.2	covered	–129.3	–139.7(12)	4.2	w
C^4–C^5–C^7–H^{7b}	113.0	106.1(10)	2.2	w	113.1	101.2(12)	2.2	w
C^4–N–C^9–H^{9a}	39.8	47.3(10)	4.2	w	39.5	46.8(12)	4.2	w
C^4–N–C^9–H^{9b}	154.8	163.4(9)	7.5	s	154.5	164.5(12)	7.5	s
C^7–N–C^8–H^{8a}	53.5	51.5(10)	2.7	w	53.7	50.7(12)	2.6	w
C^7–N–C^8–H^{8b}	172.2	169.1(9)	8.8	m	172.3	171.2(11)	8.8	m
C^9–N–C^8–H^{8a}	172.6	169.0(10)	8.8	m	172.6	169.8(12)	8.8	m
C^9–N–C^8–H^{8b}	53.9	50.3(9)	2.6	w	53.9	47.8(11)	2.6	w
C^{11}–N–C^8–H^{8a}	178.7	173.3(9)	8.9	s	178.8	173.9(12)	8.9	s
C^{11}–N–C^8–H^{8b}	–62.7	–69.0(9)	1.8	w	–62.5	–65.6(11)	1.8	w
C^{11}–N–C^7–H^{7a}	39.7	48.5(9)	4.2	w	39.6	49.5(12)	4.2	w
C^{11}–N–C^7–H^{7b}	155.0	164.5(10)	7.5	s	154.8	167.2(11)	7.5	s
C^{11}–C^{10}–C^9–H^{9a}	129.0	–133.9(9)	4.2	m	–128.6	–131.1(12)	4.1	m
C^{11}–C^{10}–C^9–H^{9b}	113.5	106.8(9)	2.2	m	114.1	111.7(11)	2.3	m

[a] PM3 optimized structure (vide infra). [b] HMBC intensity is given in the scale strong > medium > weak > null. Karplus relationship $^3J_{CH} = 3.6 \cos 2\theta - \cos\theta + 4.3$.

good agreement with the expected $^3J_{CH}$ values (Table II). In addition, there are small coupling constants between protons H^8 and H^9, and between protons H^8 and H^7; however, these rarely observed interactions were found to be useless for chemical shift assignment.

The distinguishing of *anti* diastereoisomer **4a** and *syn* diastereoisomer **4b** of unsymmetrical bis-TB derivatives based on NMR is well described[10a,12]. However, for distinguishing the isomers of symmetrical bis-TB derivatives only an empirical rule was described[7b], and applied[10b] also to tris-TB derivatives. According to the rule, the absolute differences between the chemical shifts of the geminal protons of all methylene bridges are larger for *syn* diastereoisomers than for *anti* diastereoisomers. Different anisotropy effects in the isomers are the explanation. We found that the differences are very small (<0.1 ppm) and the rule holds for isomers of **4** only in $CDCl_3$; however, it failed in other solvents (Table III). We believe that the anisotropy effects could be less important than the effects of solvent, especially when even very weak host-guest complexes are formed. On the other hand, the chemical shifts differences for H^8 protons (ca. –0.2 ppm) and also the differences for atoms H^2 ($\Delta\delta$ = 0.24–0.32), H^6 ($\Delta\delta$ = 0.34–0.50), H^{8b} ($\Delta\delta$ = 0.26–0.30) and H^{13} ($\Delta\delta$ = 0.18–0.31) as well as certain chemical shifts of carbons, in aromatic solvents (benzene-d_6, toluene-d_7, nitrobenzene-d_5) appear to be useful. Summarizing, it appears difficult to unambiguously distinguish *syn* and *anti* diastereoisomers of symmetrical bis-TB derivatives on the basis of NMR data only.

TABLE III
Chemical shift differences for hydrogens of the methylene bridge in **4**

Solvent	$\Delta\Delta\delta_{H7} = \lvert\delta_{H7a}-\delta_{H7b}\rvert^{syn} - \lvert\delta_{H7a}-\delta_{H7b}\rvert^{anti}$	$\Delta\Delta\delta_{H8} = \lvert\delta_{H8a}-\delta_{H8b}\rvert^{syn} - \lvert\delta_{H8a}-\delta_{H8b}\rvert^{anti}$	$\Delta\Delta\delta_{H9} = \lvert\delta_{H9a}-\delta_{H9b}\rvert^{syn} - \lvert\delta_{H9a}-\delta_{H9b}\rvert^{anti}$
$CDCl_3$	0.04	0.01	0.07
CD_3CN	0.01	–0.03	–0.03
C_6D_6	0.10	–0.21	0.09
$C_6D_5CD_3$	0.08	–0.22	0.09
$C_6D_5NO_2$	0.10	–0.20	0.07
CD_3NO_2	0.02	–0.07	–0.04
CF_3COOD	0.02	–0.03	–0.13

Infrared and Raman Spectroscopy

We attempted to distinguish the *anti* diastereoisomer **4a** and *syn* diastereoisomer **4b** isomers by IR and Raman spectra. In general, while the intensity of an IR absorption band depends on the change in the dipole moment during the corresponding vibrational motion, the intensity of a Raman active band depends on the change in the polarizability during that vibration. Thus, vibrational spectra are sensitive to the symmetry of molecular vibrations, which are related to the symmetry of molecules. In addition, the rule of mutual exclusion states for molecules with a center of symmetry; molecular vibrations symmetric with regard to the center of symmetry are forbidden in the IR, whereas molecular vibrations, which are antisymmetric to the centre of symmetry, are forbidden in the Raman spectrum. This rule is easy to apply to small molecules with a limited number of vibrational modes, but it is not as straightforward in the case of large molecules with many vibrational modes of similar frequencies. Furthermore, the forbidden vibrational transitions can be observed as very weak or weak bands in the corresponding spectra.

To overcome these problems and to confirm the structural difference between both isomers, we performed a detailed comparison of the precise band positions and relative intensities for both isomers in the common wavenumber range 1700–650 cm^{-1}. We sought the closest corresponding peak positions in the Raman and IR spectra measured under matching conditions (solid-state, solution) creating pairs of peak positions. We found forty such pairs in the solid-state spectra of both isomers, and 35 pairs for **4a** (36 for **4b**) in the solution spectra. For each of the pairs we calculated the absolute value of the wavenumber difference and summed these differences (Tables IV and V). The hypothesis is that the sum of differences has to be bigger for **4a** than for **4b**, because with centrosymmetric **4a** there are some similar, but not identical modes observed in IR and Raman spectra, whereas the identical modes can be observed in the case of **4b**. The result is in agreement with the hypothesis. While in the case of **4a** the sum of differences is 117 and 108 for solid-state spectrum and for spectrum in solution, respectively, in the case of **4b** the corresponding values are 85 and 69 (the difference between **4a** and **4b** is more than 30 in both cases; $(\Sigma \text{ diff (IR–Ram)}^{anti} - \Sigma \text{ diff (IR–Ram)}^{syn})_{solid} = 32$; $(\Sigma \text{ diff (IR–Ram)}^{anti} - \Sigma \text{ diff (IR–Ram)}^{syn})_{CDCl3} = 39$). Furthermore, in the case of **4a** there are bigger differences between the intensities of many bands in IR and Raman spectrum compared to those of similar intensities in the IR and Raman spectra of compound **4b**. Hence, we see that for centrosymmetric **4a** many intense

TABLE IV
The IR and Raman wavenumbers (in cm^{-1}) for *anti* diastereoisomer **4a**

IR		Raman		Diff (IR–Ram)[a]	
solid	$CDCl_3$	solid	$CDCl_3$	solid	$CDCl_3$
1610 m	1610 w	1612 m	1612 m	2	2
–	–	1594 m	1596 m	–	–
1575 w	1575 vw	1579 m	1583 m	4	8
1492 vs	1494 vs	1498 vw	1497 vw	6	3
1473 vs	1474 s	1476 sh–vw	1473 sh–vw	3	1
1464 sh	1465 sh	1463 w	1462 m	1	3
1441 sh	1443 vw	1442 sh	1443 sh	1	0
1434 m	1435 w	1436 s	1437 m	2	2
1427 sh	1425 sh	1419 sh	1421 sh	8	4
1361 w	1362 w	1356 s	1355 s	5	7
1337 vw	1338 vw	1338 w	1341 sh	1	3
1327 m	1328 w	1326 w	1328 vw	1	0
1309 m	1310 w	1313 w	1309 w	4	1
1291 w	1292 vw	1299 w	1302 sh–vw	8	10
1272 s	1273 m	1278 m	1278 m	6	5
–	–	1263 sh	1264 m	–	–
1257 s	1257 m	1259 m	1259 m	2	2
1237 s	1237 m	1238 w	1239 w	1	2
1217 s	1217 m	1206 m–w	1209 m–w	11	8
1187 s	1187 s	1191 w	1189 w	4	2
1163 sh–w	1164 sh–vw	1166 w	1167 w	3	3
1151 m	1151 m	1150 w	1153 w	1	2
1142 sh	1143 sh	1143 sh–w	1144 sh–w	1	1
–	–	1106 w	1105 sh	–	–
1094 m	1093 w	1092 m	1093 m	2	0
1076 m	1076 m	1077 w	1076 w	1	0
1038 s	1038 m	1040 w	1041 w	2	3
1022 sh–w	1022 sh–vw	1022 w	1021 w	0	1
1013 w	1012 w	1015 sh–vw	1013 sh–vw	2	1

TABLE IV
(*Continued*)

IR		Raman		Diff (IR–Ram)[a]	
solid	$CDCl_3$	solid	$CDCl_3$	solid	$CDCl_3$
997 vw	994 sh–vw	996 w	997 w	1	3
972 s	972 m	970 vw	967 vw	2	5
960 s	960 m	960 w	958 w	0	2
943 s	943 m	950 vw	947 vw	7	4
920 w	924 m	922 m–w	923 m–w	2	1
904 s	solvent	905 vw	903 vw	1	–
–	solvent	896 w	897 w	–	–
860 sh	863 w	854 w	858 vw	6	5
839 s	840 s	843 vw–sh	846 vw	4	6
824 m	824 m	827 m	825 m	3	1
806 w	806 w	812 s	813 m	6	7
749 vs	solvent	750 vw	–	1	–
735 sh	solvent	736 s	734 s	1	–
–	solvent	726 m	724 sh	–	–
719 sh	solvent	719 m–w	719 sh	0	–
681 m	680 m	–	solvent	–	–
668 m	669 m	669 m	solvent	1	–
		Number of compared items		40	35
			ΣDiff (IR–Ram)^{anti}	117	108

[a] Diff (IR–Ram) = absolute values of differences between corresponding peak positions in IR and Raman spectra.

TABLE V
The IR and Raman wavenumbers (in cm^{-1}) for *syn* diastereoisomer **4b**

IR		Raman		Diff (IR–Ram)[a]	
solid	$CDCl_3$	solid	$CDCl_3$	solid	$CDCl_3$
1611 w	1610 w	1612 sh	1612 m	1	2
–	–	1604 m	–	–	–
–	–	1598 m	1597 m	–	–
–	–	–	1588 sh	–	–
1475 w	1474 w	1473 m–s	1579 sh	2	5
1494 vs	1494 vs	1494 vw	1495 vw	0	1
1474 s	1474 s	1470 w	1475 sh–vw	4	1
1460 sh	1456 sh	1459 m–w	1456 m	1	0
1440 m	1442 sh	1439 m	1442 sh	1	0
1435 sh	1435 w	1434 sh–w	1436 m	1	1
1427 m	1427 w	1420 w	1421 sh–w	7	6
1373 vw	–	1370 m	–	3	–
1360 sh	1361 vw	1357 s	1356 vs	3	5
1342 w	1343 w	1349 sh	1347 sh	7	4
1326 w–m	1327 w	1322 m	1328 m	4	1
1310 w	1310 w	1306 w	1310 w	4	0
1291 sh–w	1292 sh–vw	1291 sh–w	1295 sh–vw	0	3
1274 m–s	1273 m	1273 m	1277 m	1	4
–	–	–	1265 m	–	–
1258 m	1256 m	1258 m–s	1258 sh	0	2
–	–	1247 m	–	–	–
1238 m	1237 m	1237 sh–w	1242 w	1	5
1213 s	1214 s	1209 m	1211 m	4	3
1188 w	1189 w	1186 w	1189 w	2	0
–	–	1179 w	–	–	–
1166 m	1166 m	1167 w	1167 w	1	1
1149 m	1150 m	1150 w	1154 w	1	4
1142 sh	1144 sh	1142 sh–vw	1143 sh	0	1
–	–	1104 w–m	1105 sh	–	–

TABLE V
(*Continued*)

IR		Raman		Diff (IR–Ram)[a]	
solid	$CDCl_3$	solid	$CDCl_3$	solid	$CDCl_3$
1092 w–m	1093 w	1092 m	1095 m	0	2
1071 m	1071 m	1070 w	1072 w	1	1
1039 m	1039 m	1043 w	1040 w	4	1
1018 w	1018 w	1020 w	1019 w	2	1
989 w	989 w	990 vw	990 vw	1	1
974 sh	974 sh–vw	974 vw	974 vw	0	0
968 m	968 m	966 vw	968 sh	2	0
948 m	950 m	949 vw	951 sh	1	1
918 w	925 w–m	916 m	924 m	2	1
902 sh	solvent	900 w	902 sh–vw	2	–
899 m	solvent	895 sh–vw	896 vw	4	–
870 sh	solvent	874 w	874 vw–sh	4	–
859 sh	863 w	–	861 vw–sh	–	2
846 sh	847 w–m	846 m	846 vw–sh	0	1
833 m–s	834 s	–	837 m	–	3
–	821 sh–w	816 m	822 w	–	1
808 sh	809 sh	807 w	805 m	1	4
–	791 sh	799 m	792 sh–vw	–	1
752 s	solvent	–	–	–	–
739 sh	solvent	738 vs	739 s	1	–
725 sh	solvent	719 sh	722 s	6	–
714 sh–w	solvent	712 s	715 sh	2	–
680 sh–w	681 sh–w	676 m–s	solvent	4	–
671 w–m	671 m	–	solvent	–	–
		Number of compared items		40	36
		ΣDiff (IR–Ram)^{anti}		85	69

[a] Diff (IR–Ram) = absolute values of differences between corresponding peak positions in IR and Raman spectra.

Raman bands are weak in the IR and vice versa, whereas such a pronounced effect is not observed in the case of **4b**. The most evident case is the band at ca. 1189 cm^{-1} attributed to a skeletal mode with considerable participation of stretching modes of C–N in the central part of the molecules[13]. This band (1187 cm^{-1}) of **4a** is strong in the IR spectrum and weak in the Raman spectrum (in both solid state and solution), while in **4b**, a weak intensity is observed in both the IR and the Raman spectrum. All of these findings show that the combination of IR and Raman spectroscopy can be a powerful tool for the structure determination of bis-TB isomers.

Furthermore, we found a striking similarity between the IR and Raman spectra obtained in the solid state and in solution for isomer **4a**, which demonstrates a negligible structural change in this molecule upon dissolution. On the other hand, evident intensity and peak position differences are observed between Raman spectra of isomer **4b** obtained in solid state and solution, suggesting some small conformational changes of isomer **4b**, which occur upon dissolution it in $CDCl_3$.

*Isomerization of Bis-TB **4***

A characteristic property of TB derivatives is racemization in acid solution. The instability in acidic media is often viewed as a disadvantage. This is true for many common TB derivatives, whereby their main applications are based on their chirality. However, in the case of bis-TB derivatives, treatment with acid may be used to control the opening and closing of the molecular tweezers. Because the behavior in acid conditions is very important for further use of bis-TB, and because it is little known about the racemization of TB[14] (only few notes[7,10,15] about oligo-TB), we performed the following studies (Table VI).

Both isomers of **4** were found to be stable in CF_3COOD at room temperature. However, above 55 °C, they isomerized rapidly. Interestingly, some tris-TB derivatives isomerize in TFA at room temperature[10a], other tris-TB derivatives are stable[10b] even at 95 °C. The ratio 4a/4b was 2:1 at equilibrium, i.e. the same ratio in which the isomers were isolated (TFA was used as the reaction solvent). We found the solvent can affects the ratio. Thus, the racemization by TFA-d_1 in toluene-d_7 gave the ratio 7:3 while in nitrobenzene-d_5 4:6. Faster isomerization of **4b** than **4a** was observed. We also observed a mild influence of the used acid. Thus, DCl in CD_3OD/D_2O led to the ratio 5:5, while CF_3COOD in CD_3OD/D_2O gave the ratio 6:4.

The isomerization in concentrated DCl (35% in D_2O) was undoubtedly the most interesting. In that case, the equilibrium is attained in 24 h at

room temperature and the ratio **4a**/**4b** was found to be 7:93. In addition, the chemical shifts of isomers **4** are very different. The ^{1}H NMR signals of isomer **4a** in are sharp and the chemical shifts are similar to those observed in CF_3COOD. In contrast, the isomer **4b** shows some very broad signals and the chemical shifts are pretty different. Together with the dramatic change in the ratio (template effect), it is obviously due to the formation of a complex of **4b** with DCl/D_2O, which is observable on NMR timescale. The biggest differences between chemical shifts ($\Delta\delta = \delta_{\mathbf{4b}} - \delta_{\mathbf{4a}}$) were observed at atoms H^6 ($\Delta\delta$ = –1.36; very broad signal), H^2 ($\Delta\delta$ = –0.82; broad signal),

TABLE VI
Isomerization equilibria of **4a** and **4b**

	Isomerization conditions				Equilibrium	
	mmol l^{-1}	acid	solvent	temp.	time	**4a**:**4b**
1	c_0(**4a**) = 2.34 c_0(**4b**) = 2.16	TFA-d_1[a]	TFA-d_1	r.t.	∞	[b]
2	c_0(**4a**) = 2.34 c_0(**4b**) = 2.16	TFA-d_1[a]	TFA-d_1	60 °C	<18 h	64:36
3	c_0(**4a**) = 0.55 c_0(**4b**) = 0.55	200 eq. DCl[c]	CD_3OD/D_2O (12:1 v/v)[d]	r.t.	~4 d	50:50
4	c_0(**4a**) = 3.02 c_0(**4b**) = 3.06	13 eq. TFA-d_1[c]	$CDCl_3$	60 °C	>10 d	69:31[e] 63:37[e]
5	c_0(**4a**) = 0.51 c_0(**4b**) = 0.52	220 eq. TFA-d_1[c]	CD_3OD	r.t.	>6 d	59:41
6	c_0(**4a**) = 0.48 c_0(**4b**) = 0.47	220 eq. TFA-d_1[c]	CD_3OD/D_2O (12:1 v/v)	r.t.	>6 d	57:43
7	c_0(**4a**) = 0.64 c_0(**4b**) = 0.64	170 eq. TFA-d_1[c]	$C_6D_5CD_3$	60 °C	<18 h	72:28
8	c_0(**4a**) = 0.64 c_0(**4b**) = 0.64	170 eq. TFA-d_1[c]	$C_6D_5NO_2$	60 °C	<18 h	41:59
9	c_0(**4a**) = 8.65 c_0(**4b**) = 8.71	DCl[a]	DCl[d]	r.t.	~24 h	7:93

[a] The acid was used as solvent. [b] No racemization. [c] eq. means equivalents of acid to a mole of **4**. [d] DCl was added as 35% (w/w) solution in D_2O. [e] The ratio at 10th day, i.e. not at equilibrium.

H^{13} ($\Delta\delta$ = –0.62), H^{7a} ($\Delta\delta$ = –0.54; broad signal) and H^3 ($\Delta\delta$ = –0.31). Despite its poor solubility, the complex is stable even in dilute acid (9% DCl in D_2O). On the other hand, no complex formation was observed in CF_3COOD over NaCl or in CF_3COOD/D_2O (1:1) over NaCl. This could be explained by different degrees of protonation. The TB systems were found to be dideuterated[14b] in solutions of strong acids such as DCl (35% in D_2O); however, based on the similarity of ^{13}C NMR spectra of **4** in CF_3COOD and of the monohydrochloride of the TB in DMSO-d_6, the TB systems of **4** are probably only monodeuterated in CF_3COOD. Unfortunately, the chemical exchanges in the system **4a**/**4b**/DCl/D_2O (deuteration, isomerization and probably also complexation) caused impossible to record complete NOESY, ^{13}C and ^{13}C correlated NMR spectra to obtain a closer view into the system. Whatever happening, the isomerization of bis-TB **4** in 35% DCl in D_2O, followed by fast neutralization and crystallization from methanol is the easy way to get pure tweezers-like isomer **4b**.

To convert **4a** to the **4b** isomer we also tried to optimize conditions of crystallization-induced asymmetric transformation (CIAT), the process we recently used for the conversion of diastereoisomers of Tröger's base derivatives[15]. Even though **4b** is less soluble (crystallizes from MeOH as the first) than **4a** in most of the solvents we used (e.g. MeOH, toluene), we did not find the conditions (solvent, concentrations, acid) where the racemization of diastereoisomers of **4** takes place in the liquid phase together with crystallization of only one diastereoisomer.

*A Note to Binding Abilities of Bis-TB **4***

The sidewalls of the tweezers **4b** are relatively flat, thus, one may not expect high binding affinity[16]. We performed titrations with potential guest molecules. By performing titrations monitored by UV-VIS spectroscopy, we found no binding of fluoranil or fullerene C_{60} to either isomer of **4**. By NMR monitoring, we found very weak and nonspecific binding of 1,2-, 1,3- and 1,4-dinitrobenzenes and 1,3,5-trinitrobenzene to both isomers of **4**. Unfortunately, due to small changes in chemical shifts ($\Delta\delta$ max ~0.07 ppm, N-CH_2-N hydrogens) and unclear stoichiometry of the weak complexes, meaningful stability constants could not be determined. We observed bigger changes in chemical shifts for **4b** compared to **4a**; however, neither three equivalents of 1,4-dinitrobenzene nor 1,3,5-trinitrobenzene has any influence on the **4a**/**4b** equilibration ratio of racemization in TFA-d_1.

In conclusion, we introduced a new member of the novel family of molecular tweezers based on Tröger's base derivatives, and showed how the ge-

ometry of the symmetrical bis-TB isomers **4** could be distinguished on the basis of IR and Raman spectra. We observed that the isomerization of bis-TB **4** in concentrated DCl (35% in D_2O) is driven by the formation a stronger complex of **4b** than of **4a**, which leads to a higher concentration of **4b** isomer in the dynamic system. It is clear that the complexation is associated with some deuteration (positive charge on nitrogen). Thus the quaternization of the nitrogens of **4**, which imports a permanent charge on the molecule, would be a way to "learn" the molecule to bind in neutral condition.

EXPERIMENTAL

Nuclear Magnetic Resonance

All NMR experiments were recorded in $CDCl_3$ solutions on a Varian Mercury instrument. ^1H and ^{13}C NMR spectra were recorded at 300.08 and 75.46 MHz, respectively. Chemical shifts δ (ppm) are referenced to the internal standard Me_4Si for both ^1H and ^{13}C NMR spectra; the coupling constants *J* are given in Hz. The correlation techniques g-HSQC, g-COSY, 2D NOESY (mixing time 450 ms) and 1D NOESY (mixing time 600 ms) were used under standard conditions. The g-HMBC spectra were recorded with parameters of $^1J_{CH}$ coupling 180 Hz (parameter j1hx) and $^nJ_{CH}$ coupling 8 Hz (parameter jnhx). The chemical shifts of the free base of diastereoisomers **4** and their coupling constants for H7a, H7b, H8a, H8b, H9a and H9b were determined by simulation as six-spins system by MestRe-C 4.4.6 (Mestrelab Research, Spain).

Raman Spectroscopy

Raman spectra (4000–100 cm^{-1}) were collected using a Fourier-transform near-infrared (FT-NIR) spectrometer Equinox 55/S (Bruker) equipped with an FT Raman module FRA 106/S (Bruker). The focused laser beam (150 mW) of a Nd:YAG laser (1064 nm, Coherent) was used to irradiate the samples studied. Both compounds *VA*-4 and *VV*-4 were examined in glass vials both in the solid state as powdered samples and in $CDCl_3$ solution. The glass vial was placed on a motor-driven X-Y-Z sample stage. The scattered light was collected in back-scattering geometry. Interferograms were obtained using a quartz beamsplitter and a Ge detector (liquid N_2 cooled). 512 and 1024 separate interferograms per 2 cm^{-1} resolved spectrum were accumulated four times and twelve times for solid samples and solutions, respectively. The data for the solvent ($CDCl_3$) were measured in the same way as for solutions. The averaged spectra and standard deviation records were calculated and saved in the JCAMP-DX format. The averaged spectrum of the solvent was subtracted from the spectra of solutions and the regions of the most intense bands of the solvent (2320–2165, 680–620, 375–350 and 271–247 cm^{-1}) were blanked. The OPUS 4.0 (Bruker) and the OMNIC 4.0 and 7.1 (Thermo Nicolet, U.S.A.) software packages were used to process the data.

Infrared Spectroscopy

IR spectra (4000–650 cm^{-1}) were collected using a FTIR spectrometer Avatar (Thermo Nicolet) equipped with single bounce ATR accessory MIRacle. The powdered samples were

placed directly on ZnSe crystal; then they were dissolved in a few droplets of $CDCl_3$ and then the solvent was left for several minutes to evaporate. Hence, a thin dry film well adhering to the ATR crystal was prepared. Afterwards 64 scans were accumulated per spectrum at 2-cm^{-1} resolution. Two repetitive measurements were performed for every sample. $CDCl_3$ was used also to clean the surface of ZnSe crystal. The same parameters were used to collect spectra of the solutions and of the solvent except for the cell, where a capped was used to prevent evaporation of the solvent. The averaged spectra were calculated and the spectrum of the solvent was subtracted from spectra of solutions. The regions of the most intense absorption bands of the solvent (915–874 and 753–690 cm^{-1}) were blanked. The OMNIC 4.0 and 7.1 (Thermo Nicolet) were used to process the spectral data.

Single-Crystal X-ray Structure Determination (**4a** and **4b**)[17]

Crystal data and details of the structure determination are presented in Table VII. Suitable single crystals were grown from methanol. A clear colorless fragment (needle) was stored under perfluorinated ether, transferred in to a Lindemann capillary, fixed, and sealed. Preliminary examination and data collection were carried out on an area detecting system (Nonius, MACH3, κ-CCD) at the window of a rotating anode (Nonius, FR951) and with graphite monochromatic MoKα radiation (λ = 0.71073 Å). The unit cell parameters were obtained by full-matrix least-squares refinement of 4091 (4201) reflections. Data collection were performed at 173 K (Oxford Cryosystems) within a θ-range of 1.92° < θ < 25.37° (1.46° < θ < 25.39°). Nine data sets were measured in rotation scan modus with Δφ/ΔΩ = 2.0° (0.70°). A total number of 24 822 (40 307) intensities were integrated. Raw data were corrected for Lorentz polarization, and for latent decay and absorption effects arising from the scaling procedure. After merging [R_{int} = 0.036 (0.046)] a sum of 4101 (3835) (all data) and 3503 (3395) [$I > 2\sigma(I)$], respectively, remained and all data were used. The structure was solved by a combination of direct methods and difference Fourier syntheses. All non-hydrogen atoms were refined with anisotropic displacement parameters. All hydrogen atom positions were found in the difference Fourier map calculated from the model containing all non-hydrogen atoms. The hydrogen positions were refined with individual isotropic displacement parameters. Full-matrix least-squares refinements with 427 (393) parameters were carried out by minimizing $\Sigma w(F_o^2 - F_c^2)^2$ with SHELXL97 weighting scheme and stopped at shift/error < 0.001. The final residual electron density maps showed no remarkable features. **4b**: The relatively high *R*-values are caused by the very low crystal quality as can be seen from the unusual high mosaicity 1.146(1)°. Neutral atom scattering factors for all atoms and anomalous dispersion corrections for the non-hydrogen atoms were taken from *International Tables for Crystallography*. All calculations were performed on an Intel Pentium II PC, with the Strux-V system, including the programs PLATON, SIR92, and SHELXL97.

CCDC 297484 (**4a**) and 297485 (**4b**) contain the supplementary crystallographic data (excluding structure factors) for this paper. These data can be obtained free of charge via www.ccdc.cam.ac.uk/conts/retrieving.html (or from the Cambridge Crystallographic Data Centre, 12, Union Road, Cambridge, CB2 1EZ, UK; fax: +44 1223 336033; or deposit@ccdc.cam.ac.uk).

N,*N*′-(1,4-Phenylene)bis(5-methoxy-2-nitrobenzamide) (**1**)

2-Nitro-5-methoxybenzoic acid (16.0 g, 81.2 mmol) was treated with thionyl chloride (12 ml) in toluene (30 ml) at 60 °C for 4 h. The resulting solution was evaporated in vacuo

TABLE VII
Summary of the crystal data and details of data collection and refinement for compounds **4a** and **4b**

Parameter	**4a**	**4b**
Empirical formula	$C_{26}H_{26}N_4O_2 \cdot CH_3OH$	$C_{26}H_{26}N_4O_2$
Formula mass	458.55	426.51
Crystal system	triclinic	monoclinic
Space group	$P\bar{1}$ (No. 2)	$P2_1/n$ (No. 14)
a, Å	9.9365(1)	16.8844(2)
b, Å	10.6602(1)	6.3595(1)
c, Å	11.61557(2)	19.7900(3)
α, °	71.1801(5)	90
β, °	74.8869(5)	100.7536(6)
γ, °	89.2167(8)	90
V, Å^3	1120.99(3)	2087.66(5)
Z	2	4
ρ_{calcd}, g cm^{-3}	1.359	1.357
μ, mm^{-1}	0.090	0.088
T, K	173	173
F(000)	488	904
Crystal size, mm	0.61 × 0.58 × 0.20	0.59 × 0.20 × 0.13
θ-range, °	1.92/25.37	1.46/25.39
Index ranges	*h*: ±11; *k*: ±12; *l*: ±13	*h*: ±20; *k*: ±7; *l*: ±23
Reflections collected	24822	40307
Independent reflections, $I_o > 2\sigma(I_o)$/all data/R_{int}	3503/4101/0.036	3395/3835/0.046
Data/restraints/parameters	4101/0/427	3835/0/393
*R*1, $I_o > 2\sigma(I_o)$/all data	0.0357/0.0442	0.0501/0.0577
*wR*2, $I_o > 2\sigma(I_o)$/all data	0.0858/0.0914	0.1264/0.1307
GOF	1.025	1.154
Weights *a*/*b*	0.0452/0.3865	0.0617/0.9483
$\Delta\rho_{max/min}$, e Å^{-3}	0.21/–0.21	0.24/–0.22

to dryness, and the residue, crude 2-nitro-5-methoxybenzoyl chloride, was dissolved in DMF (40 ml). A solution of 1,4-diaminobenzene (3.5 g, 32.4 mmol) in pyridine (20 ml) was added over 10 min. The reaction mixture was stirred at room temperature overnight and then at 45 °C for 3 h. The solution was diluted with water (1 l), and the precipitated product was filtered off, and washed with water, methanol and dichloromethane. After drying in vacuo 14.9 g (99%) of **1** was obtained. M.p. 296–298 °C. ^{1}H NMR (300 MHz, DMSO-d_6): 10.58 br s, 2 H (NH); 8.18 d, 2 H, $^3J_{HH}$ = 8.8; 7.23 m, 4 H; 7.65 s, 4 H; 3.94 s, 6 H (OCH_3). ^{13}C APT NMR (75 MHz, DMSO-d_6): 163.8 (C), 163.5 (C), 138.7 (C), 135.7 (C), 134.9 (C), 127.0 (CH), 120.0 (2 × CH), 115.4 (CH), 114.2 (CH), 56.6 (OCH_3). For $C_{22}H_{18}N_4O_8$ (466.4) calculated: 56.66% C, 3.89% H, 12.01% N; found: 56.24% C, 3.91% H, 12.07% N. LRMS (FAB$^+$): 467 (100%, MH^+), 436 (50%, $MH^+ - OCH_3$).

N,*N*′-(1,4-Phenylene)bis(2-amino-5-methoxybenzamide) (**2**)

A flask was charged with compound **1** (13.6 g, 29.2 mmol), catalyst (5% Pd/C, 1.3 g), methanol (30 ml) and DMF (50 ml). The reaction mixture was stirred for 2 days under hydrogen. The catalyst was filtered off under argon and the solvent evaporated in vacuo. The residue was washed with toluene (100 ml) to give **2** (10.8 g, 91%). M.p. 214–217 °C. ^{1}H NMR (DMSO-d_6): 10.00 s, 2 H (NH); 7.66 s, 4 H; 7.18 d, 2 H, $^4J_{HH}$ = 3.0; 6.91 dd, 2 H, $^3J_{HH}$ = 8.9, $^4J_{HH}$ = 3.0; 6.72 d, 2 H, $^3J_{HH}$ = 8.8; 5.75–6.10 m, 4 H (NH_2); 3.73 s, 6 H (OCH_3). ^{13}C APT NMR (DMSO-d_6): 167.3 (CO), 149.4 (C), 143.7 (C), 134.8 (C), 120.9 (2 × CH), 119.7 (CH), 117.9 (CH), 115.8 (C), 112.6 (CH), 55.6 (OCH_3). For $C_{22}H_{22}N_4O_4$ (406.5) calculated: 65.01% C, 5.46% H, 13.78% N; found: 64.64% C, 5.80% H, 13.64% N. LRMS (FAB$^+$): 407 (25%, MH^+), 157 (5%, $MH^+ - C_8H_8NO_2$), 150 (100%, $C_8H_8NO_2^+$).

N,*N*′-Bis(2-amino-5-methoxybenzyl)-1,4-phenylenediamine (**3**)

A 3 M toluene solution of LAH (50 ml, 150 mmol) was slowly added to a solution of **2** (4.00 __, 9.85 mmol) in dioxane (40 ml). The reaction mixture was refluxed for 8 h, cooled and carefully quenched with water (12 ml), 15% aqueous solution of NaOH (14 ml) and water (14 ml). The insoluble part was filtered off and washed with dioxane (2 × 30 ml) and diethyl ether (4 × 30 ml). The light brown compound **3** (3.6 g, 97%) was obtained from the filtrate by evaporation to dryness in vacuo. ^{1}H NMR (DMSO-d_6): 6.72 m, 2 H; 6.57 m, 4 H; 6.46 s, 4 H; 5.14 t, 2 H, $^3J_{HH}$ = 5.6 (NH); 4.54 s, 4 H (NH_2); 3.94 d, 4 H, $^3J_{HH}$ = 5.5 (CH_2); 3.59 s, 6 H (OCH_3). ^{13}C APT NMR (DMSO-d_6): 150.9 (C), 140.5 (C), 140.0 (C), 125.1 (C), 115.6 (CH), 114.3 (CH), 114.0 (2 × CH), 112.3 (CH), 55.2 (OCH_3), 45.2 (CH_2).

3,12-Dimethoxy-16,17-dihydro-5*H*,10*H*-6,18:9,15-dimethanobenzo[1,2-*c*:6,5-*c*′]-bis[1,5]benzodiazocine **4a** and **4b**

Compound **3** (3.10 g, 8.19 mmol) and hexamethyltetramine (3.3 g, 23.57 mmol) were added to trifluoroacetic acid (130 ml). The reaction mixture was stirred at 60 °C for 12 h, then diluted with water (1 l) and ice, alkalinized with concentrated ammonia solution, and extracted with dichloromethane (3 × 200 ml). The organic layers were combined, washed with brine, dried over anhydrous Na_2SO_4 and evaporated in vacuo to dryness. The residue was separated by column chromatography (silica, dichloromethane/methanol 95:5). As the first isomer **4a** (890 mg, 25%) was eluted, followed by isomer **4b** (520 mg, 15%).

(6R,9R*,15R*,18R*)-3,12-Dimethoxy-16,17-dihydro-5H,10H-6,18:9,15-dimethanobenzo-[1,2-c:6,5-c′]bis[1,5]benzodiazocine* (**4a**). ^{1}H NMR ($CDCl_3$): 6.98 d, 2 H, $^3J_{HH}$ = 8.8 (H^3, H^{16}); 6.90 s, 2 H (H^{12}, H^{25}); 6.67 dd, 2 H, $^3J_{HH}$ = 8.8, $^4J_{HH}$ = 2.8 (H^2, H^{15}); 6.35 d, 2 H, $^4J_{HH}$ = 2.8 (H^6, H^{19}); 4.54 d, 2 H, $^2J_{HH}$ = 16.6 (H^{7b}, H^{20b}); 4.22 d, 2 H, $^2J_{HH}$ = 16.7 (H^{9b}, H^{22b}); 4.13 d, 2 H, $^2J_{HH}$ = 12.4 (H^{8a}, H^{21a}); 4.05 d, 2 H, $^2J_{HH}$ = 12.4 (H^{8b}, H^{21b}); 4.04 d, 2 H, $^2J_{HH}$ = 16.6 (H^{7a}, H^{20a}); 3.73 d, 2 H, $^2J_{HH}$ = 16.7 (H^{9a}, H^{22a}); 3.62 s, 6 H (H^{13}, H^{26}). ^{13}C NMR ($CDCl_3$): 156.1 (C^1, C^{14}), 143.7 (C^{11}, C^{24}), 140.9 (C^4, C^{17}), 128.7 (C^5, C^{18}), 126.0 (C^3, C^{16}), 124.9 (C^{10}, C^{23}), 124.2 (C^{12}, C^{25}), 113.9 (C^2, C^{15}), 110.8 (C^6, C^{19}), 66.3 (C^8, C^{21}), 58.4 (C^7, C^{20}), 55.8 (C^9, C^{22}), 55.3 (C^{13}, C^{26}). For atom numbering, see Fig. 1 and for chemical shifts in other solvents, see Tables VIII and IX. M.p. 254–258 °C with decomposition. For $C_{26}H_{26}N_4O_2$ (426.5) calculated: 73.22% C, 6.14% H, 13.14% N; found: 72.85% C, 6.20% H, 12.90% N. HRMS (FAB^+): for $C_{26}H_{26}N_4O_2$ (MH^+) calculated: 427.2134; found: 427.2124.

(6R,9S*,15S*,18R*)-3,12-dimethoxy-16,17-dihydro-5H,10H-6,18:9,15-dimethanobenzo-[1,2-c:6,5-c′]bis[1,5]benzodiazocine* (**4b**). ^{1}H NMR ($CDCl_3$): 6.94 d, 2 H, $^3J_{HH}$ = 8.8 (H^3, H^{16}); 6.91 s, 2 H (H^{12}, H^{25}); 6.61 dd, 2 H, $^3J_{HH}$ = 8.8, $^4J_{HH}$ = 2.9 (H^2, H^{15}); 6.32 d, 2 H, $^4J_{HH}$ = 2.9 (H^6, H^{19}); 4.56 d, 2 H, $^2J_{HH}$ = 16.8 (H^{7b}, H^{20b}); 4.28 d, 2 H, $^2J_{HH}$ = 17.0 (H^{9b}, H^{22b}); 4.11 d, 2 H, $^2J_{HH}$ = 12.6 (H^{8a}, H^{21a}); 4.02 d, 2 H, $^2J_{HH}$ = 16.8 (H^{7a}, H^{20a}); 4.02 d, 2 H, $^2J_{HH}$ = 12.6 (H^{8b}, H^{21b}); 3.72 d, 2 H, $^2J_{HH}$ = 17.0 (H^{9a}, H^{22a}); 3.59 s, 6 H (H^{13}, H^{26}). ^{13}C NMR ($CDCl_3$): 156.1 (C^1, C^{14}), 143.7 (C^{11}, C^{24}), 141.1 (C^4, C^{17}), 128.7 (C^5, C^{18}), 126.2 (C^3, C^{16}), 124.7 (C^{10}, C^{23}), 124.1 (C^{12}, C^{25}), 113.9 (C^2, C^{15}), 110.7 (C^6, C^{19}), 66.4 (C^8, C^{21}), 58.1 (C^7, C^{20}), 55.8 (C^9, C^{22}), 55.3 (C^{13}, C^{26}). For atom numbering, see Fig. 1 and for chemical shifts in other solvents, see Tables VIII and IX. M.p. 271–281 °C with decomposition. For $C_{26}H_{26}N_4O_2$ (426.5) calculated: 73.22% C, 6.14% H, 13.14% N; found: 72.68% C, 6.26% H, 12.96% N. HRMS (FAB^+): for $C_{26}H_{26}N_4O_2$ (MH^+) calculated: 427.2134; found: 427.2124.

One-Pot Preparation of **4a** and **4b**

A vial was charged with 1,4-phenylenediamine (105 mg, 0.97 mmol), 4-methoxyaniline (344 mg, 2.79 mmol) and hexamethylenetetramine (260 mg, 1.85 mmol), and TFA (4 ml) was added. The mixture was stirred at 80 °C for 18 h. After cooling the mixture was treated with methylene chloride and water, and neutralized by adding solid $NaHCO_3$, and alkalized by adding concentrated aqueous ammonia. The aqueous layer was extracted with CH_2Cl_2, the combined organic layers were dried over anhydrous Na_2SO_4 and evaporated to dryness in vacuo. The complex mixture was separated by repeated column chromatography on silica using a CH_2Cl_2/methanol mixture (from 1:0 to 9:1) to obtain 9 mg (2%) of formyl-TB **7**, 74 mg (19%) of mono-TB **6** and 29 mg (7%) of bis-TB **4** (**4a**/**4b** 2:1).

2,8-Dimethoxy-6H,12H-5,11-methanodibenzo[b,f][1,5]diazocine-4-carbaldehyde (**7**). ^{1}H NMR ($CDCl_3$): 10.57 s, 1 H (H^{18}); 7.22 d, 1 H, $^4J_{HH}$ = 3.0 (H^{13}); 7.08 d, 1 H, $^3J_{HH}$ = 8.8 (H^3); 6.77 dd, 1 H, $^3J_{HH}$ = 8.8, $^4J_{HH}$ = 2.9 (C^2); 6.71 d, 1 H, $^4J_{HH}$ = 3.0 (H^{15}); 6.41 d, 1 H, $^4J_{HH}$ = 2.9 (H^6); 4.80 d, 1 H, $^2J_{HH}$ = 16.8 (H^{7b}); 4.69 d, 1 H, $^2J_{HH}$ = 16.8 (H^{9b}); 4.35 d, 1 H, $^2J_{HH}$ = 12.8 (H^8); 4.34 d, 1 H, $^2J_{HH}$ = 12.8 (H^8); 4.14 d, 1 H, $^2J_{HH}$ = 16.8 (H^{9a}); 3.97 d, 1 H, $^2J_{HH}$ = 16.8 (H^{7a}); 3.75 s, 3 H (H^{16}); 3.70 s, 3 H (H^{17}). ^{13}C NMR ($CDCl_3$): 190.9 (C^{18}), 156.3 (C^1), 155.9 (C^{14}), 144.6 (C^{11}), 140.6 (C^4), 130.3 (C^{10}), 128.1 (C^5), 126.1 (C^3), 122.5 (C^{12}), 119.6 (C^{15}), 114.4 (C^2), 110.8 (C^{13}), 110.5 (C^6), 67.0 (C^8), 60.5 (C^7), 58.4 (C^9), 55.5 (C^{16}), 55.4 (C^{17}). For atom numbering, see Chart 1. HRMS (FAB^+): for $C_{18}H_{19}N_2O_3$ (MH^+) calculated: 311.1396; found: 311.1396.

TABLE VIII
^{13}C NMR chemical shifts (in ppm) for **4a** and **4b** in various solvents

Carbon		$CDCl_3$	CD_3NO_2	C_6D_6	$C_6D_5CD_3$	$C_6D_5NO_2$	CF_3COOD
C^1	**4a**	156.10	157.48	157.04	156.99	156.58	161.11
	4b	156.06	157.40	156.64	156.71	156.18	160.94
C^2	**4a**	113.88	115.09	114.62	114.47	114.24	116.57
	4b	113.85	114.91	114.59	114.60	113.81	116.25
C^3	**4a**	126.00	127.31	126.82	126.76	126.64	125.30
	4b	126.17	127.32	126.36	126.44	126.57	125.41
C^4	**4a**	140.91	142.71	142.66	142.68	142.15	129.57
	4b	141.13	142.57	142.27	142.36	141.84	129.69
C^5	**4a**	128.65	130.56	129.77	129.75	~129.55	127.50
	4b	128.72	130.54	129.11	~129.30	~129.25	127.73
C^6	**4a**	110.79	111.97	111.61	111.54	111.14	113.37
	4b	110.66	111.91	111.24	111.03	110.56	113.07
C^7	**4a**	58.43	59.54	59.31	59.34	59.12	57.22
	4b	58.06	59.39	59.06	59.15	59.13	56.77
C^8	**4a**	66.34	67.58	67.08	67.07	67.14	68.23
	4b	66.44	67.68	67.45	67.43	67.27	68.36
C^9	**4a**	55.80	56.79	56.64	56.66	56.42	56.10
	4b	55.77	56.87	56.88	56.88	56.44	55.95
C^{10}	**4a**	124.90	126.74	125.88	~125.81	126.08	120.98
	4b	124.74	126.53	125.74	~125.68	126.17	120.80
C^{11}	**4a**	143.67	145.27	144.89	144.96	144.88	140.98
	4b	143.71	145.15	145.07	145.07	145.07	141.10
C^{12}	**4a**	124.20	125.34	124.93	124.90	124.94	126.98
	4b	124.10	125.21	124.90	124.89	124.90	127.00
C^{13}	**4a**	55.27	56.03	55.31	55.17	55.26	55.89
	4b	55.25	55.90	54.93	54.83	54.83	55.74

Table IX
^{1}H NMR chemical shifts (in ppm, followed by J_{HH} in Hz) for **4a** and **4b** in various solvents

Hydrogen		$CDCl_3$	CD_3CN	CD_3NO_2	C_6D_6	$C_6D_5CD_3$	$C_6D_5NO_2$	DCl in D_2O	CF_3COOD
H^2	**4a**	6.67, 8.8, 2.8	6.73, 8.8, 2.8	6.74, 8.8, 2.9	6.75, 8.7, 2.9	6.62, 8.7, 2.8	6.70, 8.7, 2.7	6.15, 9.1, 2.7	7.03, 9.1, 2.7
	4b	6.61, 8.8, 2.9	6.65, 8.8, 2.9	6.61, 8.8, 2.9	6.47, 8.7, 2.9	6.38, 8.7, 2.7	6.38, 8.7, 2.7	5.34, br d	6.85, 9.0, 2.5
H^3	**4a**	6.98, 8.8	7.02, 8.8	7.05, 8.8	7.08, 8.7	6.98, 8.7	7.13, 8.7	6.70, 9.1	7.47, 9.1
	4b	6.94, 8.8	6.96, 8.8	6.96, 8.8	6.92, 2.9	6.81, 8.7	6.96, 8.7	6.39, 9.0	7.34, 9.0
H^6	**4a**	6.35, 2.8	6.48, 2.8	6.50, 2.9	6.26, 2.9	6.15, 2.8	6.29, 2.7	5.87, br s	6.75, 2.7
	4b	6.32, 2.9	6.42, 2.9	6.40, 2.9	5.90, 8.7	5.81, 2.7	5.79, 2.7	4.51, very br s	6.59, 2.5
H^{7a}	**4a**	4.04, 16.6	4.06, 16.9	4.12, 16.8	3.96, 16.8, 1.6	3.87, 16.7, 1.7	4.17, 16.7	3.75, 17.1	4.45, 17.4
	4b	4.02, 16.8	4.04, 16.8	4.09, 16.9	3.83, 16.6	3.76, 16.7	3.99, 16.8	3.21, br d	4.35, 17.4
H^{7b}	**4a**	4.54, 16.6	4.54, 16.9	4.56, 16.8	4.34, 16.8	4.26, 16.7	4.56, 16.7	4.17, 17.1	4.93, 17.4
	4b	4.56, 16.8	4.53, 16.8	4.55, 16.9	4.31, 16.6	4.23, 16.7	4.48, 16.8	3.88, 17.2	4.85, 17.4
H^{8a}	**4a**	4.13, 12.4	4.14, 12.2	4.15, 12.5, 1.2	3.99, 12.6, 1.6	3.88, 12.8, 1.5	4.13, 12.6	4.40, 11.5	5.11, 11.9
	4b	4.11, 12.6	4.15, 12.4	4.15, 12.5	4.08, 12.5	3.98, 12.4	4.19, 12.4	4.26, 11.7	5.06, 11.7
H^{8b}	**4a**	4.05, 12.4	4.06, 12.2	4.06, 12.5, 1.7	3.76, 12.6, 1.6	3.64, 12.8, 1.7	3.90, 12.6	4.03, 11.5	4.84, 11.9
	4b	4.02, 12.6	4.10, 12.4	4.17, 12.5	4.06, 12.5	3.96, 12.4	4.16, 12.4	4.09, 11.7	4.82, 11.7
H^{9a}	**4a**	3.73, 16.7	3.80, 17.0	3.89, 17.1	3.68, 16.6, 1.6	3.60, 16.6, 1.5	4.03, 16.8	3.60, 16.2	4.38, 16.0
	4b	3.72, 17.0	3.81, 16.9	3.92, 17.1	3.83, 16.8	3.71, 16.8	4.22, 17.0	3.53, 16.4	4.44, 16.5
H^{9b}	**4a**	4.22, 16.7	4.28, 17.0	4.32, 17.1	3.90, 16.6	3.86, 16.6	4.36, 16.8	4.31, 16.2	5.06, 16.0
	4b	4.28, 17.0	4.26, 16.9	4.31, 17.1	4.14, 16.8	4.05, 16.8	4.42, 17.0	4.20, 16.2	4.99, 16.5
H^{12}	**4a**	6.90	6.94	6.97	7.02	6.91	7.14	6.83	7.50
	4b	6.91	6.95	7.00	7.07	6.95	7.20	6.91	7.46
H^{13}	**4a**	3.62	3.67	3.69	3.25	3.20	3.60	2.89	3.84
	4b	3.59	3.61	3.59	3.07	3.00	3.29	2.27	3.71

Reaction of Amines in with Paraformaldehyde in the Melt

A vial was charged with 4-methoxyaniline (114 mg, 0.93 mmol), 1,4-phenylenediamine (50 mg, 0.46 mmol), paraformaldehyde (84 mg) and $TsOH \cdot H_2O$ (257 mg, 1.35 mmol), tightly closed and heated at 80 °C in an oil bath for 17 h. The obtained melt was treated with a mixture of concentrated aqueous ammonia (1 ml), CH_2Cl_2 (30 ml), and water (25 ml). The organic layer was dried over anhydrous $MgSO_4$ and evaporated to dryness. The obtained solid was separated by preparative TLC (20 × 20 × 0.2 cm, silica, Uniplate, AnalTech, 3% of CH_3OH in CH_2Cl_2) to obtain 25 mg (20%) of **8**. When the experiment was repeated without 1,4-phenylenediamine, a 22% yield of **8** was obtained.

6-Methoxy-3-(4-methoxyphenyl)-3,4-dihydroquinazoline (**8**). ^{1}H NMR ($CDCl_3$): 7.37 s, 1 H (H^2); 7.13 d, 1 H, $^3J_{HH}$ = 8.6 (H^8); 7.10 d, 2 H, $^3J_{HH}$ = 9.0 (H^{13}); 6.94 d, 2 H, $^3J_{HH}$ = 9.0 (H^{14}); 6.78 dd, 1 H, $^3J_{HH}$ = 8.6, $^4J_{HH}$ = 2.8 (H^7); 6.51 d, 1 H, $^4J_{HH}$ = 2.8 (H^5); 4.87 s, 2 H (H^4); 3.82 s, 3 H (H^{16}); 3.78 s, 3 H (H^{11}). ^{13}C NMR ($CDCl_3$): 157.5 (C^6), 156.8 (C^{15}), 145.7 (C^2), 136.8 (C^{12}), 134.6 (C^{10}), 125.6 (C^8), 122.0 (C^9), 120.1 (C^{13}), 114.7 (C^{14}), 113.3 (C^7), 111.1 (C^5), 55.5 (C^{16}), 55.4 (C^{11}), 47.7 (C^4). For atom numbering, see Chart 1. HRMS (FAB$^+$): for $C_{16}H_{17}N_2O_2$ (MH^+) calculated: 269.1290; found: 269.1290.

This work was supported by the Ministry of Education, Youth and Sports of the Czech Republic (MSM 6046137307 and LC06077), Grant Agency of the Czech Republic (203/03/D049), and EU (CIDNA NMP4-CT-2003-505669).

REFERENCES

1. Tröger J.: *J. Prakt. Chem.* **1887**, *36*, 225.
2. Spielman M. A.: *J. Am. Chem. Soc.* **1935**, *57*, 583.
3. a) Bag B. G.: *Curr. Sci.* **1995**, *68*, 279; b) Demeunynck M., Tatibouet A. in: *Progress in Heterocycles Chemistry* (G. W. Gribble and T. L. Cilchrist, Eds), p. 1–20. Pergamon, Oxford 1999.
4. a) Goswami S., Ghosh K., Dasgupta S.: *J. Org. Chem.* **2000**, *65*, 1907; b) Hansson A. P., Norrby P.-O., Wärnmark K.: *Tetrahedron Lett.* **1998**, *39*, 4565; c) Wilcox C. S., Greer L. M., Lynch V.: *J. Am. Chem. Soc.* **1987**, *109*, 1865.
5. a) Allen P. R., Reek J. N. H., Try A. C., Crossley M. J.: *Tetrahedron: Asymmetry* **1997**, *8*, 1161; b) Webb T. H., Suh H., Wilcox C. S.: *J. Am. Chem. Soc.* **1991**, *113*, 8554; c) Wilcox C. S., Adrian J. C., Webb T. H., Zawacki F. J.: *J. Am. Chem. Soc.* **1992**, *114*, 10189.
6. a) Baldeyrou B., Tardy C., Bailly C., Colson P., Houssier C., Charmantray F., Demeunynck M.: *Eur. J. Med. Chem.* **2002**, *37*, 315; b) Johnson R. A., Gorman R. R., Wnuk R. J., Crittenden N. J., Aiken J. W.: *J. Med. Chem.* **1993**, *36*, 3202; c) Bailly C., Laine W., Demeunynck M., Lhomme J.: *Biochem. Biophys. Res. Commun.* **2000**, *273*, 681.
7. a) Pardo C., Sesmilo E., Gutierrez-Puebla E., Monge A., Elguero J., Fruchier A.: *J. Org. Chem.* **2001**, *66*, 1607; b) Mas T., Pardo C., Salort F., Elguero J., Torres M. R.: *Eur. J. Org. Chem.* **2004**, 1097.
8. Valík M., Dolenský B., Petříčková H., Král V.: *Collect. Czech. Chem. Commun.* **2002**, *67*, 609.
9. Dolenský B., Valík M., Sýkora D., Král V.: *Org. Lett.* **2005**, *7*, 67.

10. a) Hansson A., Wixe T., Bergquist K.-E., Wärnmark K.: *Org. Lett.* **2005**, *7*, 2019; b) Artacho J., Nilsson P., Bergquist K.-E., Wendt O. F., Wärnmark K.: *Chem. Eur. J.* **2006**, *12*, 2692.
11. Wagner E. C.: *J. Org. Chem.* **1937**, *2*, 157.
12. a) Cudero J., Jiménez P., Marcos C., Pardo C., Ramos M., Elguero J., Fruchier A.: *Magn. Reson. Chem.* **1996**, *34*, 318; b) Pardo C., Ramos M., Fruchier A., Elguero J.: *Magn. Reson. Chem.* **1996**, *34*, 708; c) Elguero J., Fruchier A., Mas T., Pardo C.: *Magn. Reson. Chem.* **2005**, *43*, 665.
13. *SpecTool 2.1, A Hypermedia Book for Structure Elucidation of Organic Compounds with Spectroscopic Methods*. Chemical Concepts GmbH, Weinheim 1994.
14. a) Prelog V., Wieland P.: *Helv. Chim. Acta* **1944**, *27*, 1127; b) Greenberg A., Molinaro N., Lang M.: *J. Org. Chem.* **1984**, *49*, 1127; c) Trapp O., Schurig V.: *J. Am. Chem. Soc.* **2000**, *122*, 1424; d) Trapp O., Trapp G., Kong J., Hahn U., Vögtle F., Schurig V.: *Chem. Eur. J.* **2002**, *8*, 3629.
15. Valík M., Dolenský B., Herdtweck E., Král V.: *Tetrahedron: Asymmetry* **2005**, *16*, 1969.
16. a) Harmata M.: *Acc. Chem. Res.* **2004**, *37*, 862; b) Klärner F.-G., Kahlert B.: *Acc. Chem. Res.* **2003**, *36*, 919; c) Klärner F.-G., Burkert U., Kamieth M., Boese R.: *J. Phys. Org. Chem.* **2000**, *13*, 604.
17. a) Data Collection Software for NONIUS κ-CCD Devices, Delft 1997; b) Otwinowski Z., Minor W.: *Methods Enzymol.* **1997**, *276*, 307; c) Hahn Th., Wilson A. J. C. (Eds): *International Tables for Crystallography*. Kluwer Academic Publisher, Dordrecht, Boston, London 1992; d) Artus G., Scherer W., Priermeier T., Herdtweck E.: *STRUX-V, A Program System to Handle X-Ray Data*. TU München, Garching 1997; e) Spek A. L.: *PLATON, A Multipurpose Crystallographic Tool*. Utrecht University, Utrecht 2001; f) Altomare A., Cascarano G., Giacovazzo C., Guagliardi A., Burla M. C., Polidori G., Camalli M.: *SIR92*; *J. Appl. Crystallogr.* **1994**, *27*, 435; g) Sheldrick G. M.: *SHELXL97*. University of Göttingen, Göttingen 1998.